Journal of the Korean Crystal Growth and Crystal Technology
Vol. 13, No. 4 (2003) 187-198

Convection in the growth of zinc telluride single crystal by physical vapor transport

Geug-Tae Kim†

Department of Chemical Engineering, Hannam University 133 Ojung-Dong, Taejon 306-791, Korea

(Received April 7, 2003)
(Accpeted July 5, 2003)

Abstract Zinc selenide (ZnSe) single crystals hold promise for many electro-optics, acousto-optic and green laser generation applications. This material is prepared in closed ampoules by the physical vapor transport (PVT) growth method based on the dissociative sublimation. We investigate the effects of diffusive-convection on the crystal growth rate of ZnSe with a low vapor pressure system in a horizontal configuration. Our results show that for the ratios of partial pressures, s = 0.2 and 2.9, the growth rate increases with the Peclet number and the temperature differences between the source and crystal. As the ratio of partial pressures approaches the stoichiometric value of 2, the rate increases. The mass flux based on one dimensional (1D model) flow for low vapor pressure system fall within the range of the predictions (2D model) obtained by solving the coupled set of conservation equations, which indicates the flow fields would be advective-diffusive. Therefore, the rate and the flow fields are independent of gravity acceleration levels.

Key words Convection, Zinc telluride, Zinc selenide, Physical vapor transport, Vapor-crystal growth

1. Introduction

The wide-bandgap II-VI compounds hold promise for blue-light emitting diodes and laser diodes. Zinc selenide (ZnSe) with a bandgap of 2.72 eV is one of the most promising materials for laser cathode-ray tube emitting in the blue range and other e-beam pumped semiconductors, so there is growing in much interest and a constant demand for a photorefractive material for optical data processing [1, 2]. Although polycrystalline ZnSe will continue to be adequate for many applications, single crystals of high quality will be required for use in optoelectronic devices. Laser diodes have been fabricated on GaAs substrates since it is difficult to obtain ZnSe single crystals of high quality for substrates. However, in the epitaxial system ZnSen-GaAs, significant biaxial strain is introduced because of the lattice mismatch and different thermal expansion coefficients. To overcome these difficulties homoepitaxy should be applied with ZnSe substrates [3]. Recent progress in II-VI device technology with the fabrication of blue-green ZnSe-based laser diodes has been based on successful electrical control of the epitaxial layers [4, 5].

ZnSe single crystals have been grown from the melt and from solution [6-10], as well as from the vapor phase by either chemical vapor transport (CVT) [11-13] or physical vapor transport (PVT) [14-19]. In this study the crystal growth method used was PVT in sealed quartz ampoules due to its high melting point (1568 K). PVT has the advantage of requiring lower temperatures than growth from the melt and it thus makes the process more amenable in instances as well as less vulnerable to contamination and the severe strains resulting from growth at very high temperatures. Lower temperature growth also reduces the potential for altering the stoichiometry of the material. Other benefits stem from the inherent purification mechanism in the process due to differences in the vapor pressures of the native elements and impurities, and the enhanced solid-vapor interfacial morphological stability during the growth process, which has been described by Rosenberger [20]. Further, the implementation of physical vapor transport (PVT) growth in closed ampoules affords experimental simplicity with minimal needs for complex process control which makes it an ideal candidate for space investigations in systems where gravity tends to have undesirable effects on the growth process. PVT is less complex than growth by chemical vapor transport (CVT) and it avoids the problem of contamination of the growing crystal by the transport agent.

It has been shown [21-23] that vapor-phase composition during physical vapor transport (PVT) growth of II-VI semiconductors has a significant effect on mass transport and hence allows a control of the growth rate.

†Corresponding author
Tel: +82-42-629-7984
Fax: +82-42-623-9489
E-mail: gtkim@mail.hannam.ac.kr

Our interest is to investigate the effects of advective-diffusion and diffusive-convection on the ZnSe crystal growth processes during physical vapor transport (PVT) based on dissociative sublimation-condensation for a parametric range corresponding to actual experimental conditions. In other words, in the PVT system of ZnSe, the molecular species ZnSe is dissociatively sublimed into the gas of the Zn (g) and Se_2 (g) in the vapor phase from the crystalline system phase ZnSe(s), and is subsequently transported and re-incorporated into the single crystalline phase (ZnSe) [24]. The influence of a residual gas is included in the two-dimensional model. The simulations show that the Stefan flux dominates the system and subtle gravitational effects can be gauged by subtracting this flux from the calculated flow fields.

Markham, Greenwell and Rosenberger [25] examined the effects of thermal and thermosolutal convections on congruent transport of species during the PVT process inside vertical cylindrical enclosures for a time-independent system, and showed that even in the absence of gravity, convection can be present, causing nonuniform concentration gradients. They emphasized the role of geometry in the analysis of the effects of convection. As such these fundamentally constitute steady state two-dimensional models. The steady state models are limited to low Rayleigh number applications, because as the Rayleigh number increases oscillation of the flow field occurs. To address the issue of unsteady flows in PVT, Duval [26] performed a numerical study on transient thermal convection for a vertical rectangular enclosure with insulated temperature boundary conditions for Rayleigh numbers up to 10^6. Duval [27] has also shown the bifurcation sequences which lead to chaotic flow in PVT processing. Duval [27, 28] used a particular material of mercurous chloride with a high vapor pressure system for practical conditions of crystal growth. Nadarajah *et al.* [29] addressed the effects of solutal convection for any significant disparity in the molecular weights of the crystal components and the inert gas. Rosenberger et al. [30] studied three-dimensional numerical modeling of the PVT yielded quantitative agreement with measured transport rates of iodine through octofluorocyclobutane (C_4F_8) as inert background gas in horizontal cylindrical ampoules. The effects of thermal convection on the growth rate of mercurous halide (Hg_2Cl_2, Hg_2Br_2) for various convective parameters such as the temperature difference, inert gases, gravitational levels, configuration, wall boundary conditions have reported [31, 32]. Up to now the previous works are concerned with the effects of convection on congruent transport. In recent years Zhou *et al.* [33] and Ramachandran *et al.* [34] addressed the effect of thermal-solutal convection non-congruent transport by dissociative sublimation-condensation. Zhou *et al.* [33] reported that the traditional approach of calculating the mass flux assuming one-dimensional flow for low vapor pressure systems such as ZnTe is indeed correct.

The main purposes of this paper are to discuss the development of a mathematical model for single crystals inside a PVT reactor, incorporating the mass transfer-limited model with idealized boundary conditions, and to predict numerically simulated transport rate for practical growth conditions of ZnSe with a low vapor system by dissociative sublimation, and to relate the applied convective process parameters to crystal growth rate. We believe the results obtained here will be helpful for proper design of experimental conditions during the PVT of ZnSe by dissociative sublimation.

2. Physical Formulation

We consider our study for the effects of advective-diffusion and/or convection on the crystal growth rate of ZnSe and its distribution across an interface. In this numerical study, a two-dimensional model is used for the analysis of the PVT processes during vapor-growth of ZnSe single crystals in horizontally oriented, closed ampoules in a two-zone furnace. Consider a rectangular enclosure of height H and transport length L, shown in Fig. 1. The source is maintained at a temperature T_s, while the growing crystal is at a temperature T_c, with $T_s > T_c$. The source material ZnSe is sublimated at x = 0 to form a single crystal at x = L. Since we consider the growth of crystals by dissociative sublimation, the binary compound ZnSe is assumed to obey the following reaction [24]:

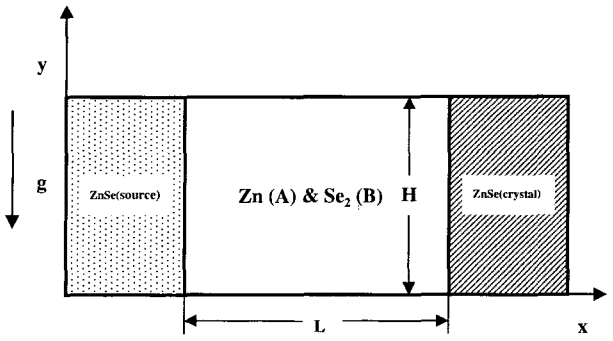

Fig. 1. Schematic representation of the PVT growth reactor in a two-dimensional rectangular system.

$$ZnSe\ (s) = Zn\ (g) + \frac{1}{2}Se_2\ (g). \quad (1)$$

Thermodynamic equilibrium conditions at interfaces are as follows:

$$P_{Zn}(0)P_{Se_2}^{1/2}(0) = K_p(T_s) \quad \text{at } x = 0, \quad (2)$$

$$P_{Zn}(L)P_{Se_2}^{1/2}(L) = K_p(T_c) \quad \text{at } x = L. \quad (3)$$

The equilibrium constant $K_p = P_{Zn}P_{Se_2}^{1/2}$ [35] for reaction (1) at temperature T is

$$\log_{10}P_{Zn}P_{Se_2}^{1/2}(T) = -18900/T + 10.003\ (atm). \quad (4)$$

$$\text{The } K_p \text{ can be expressed as } RT\ln(P_{Zn}P_{Se_2}^{1/2}) = -361807 + 191.485T\ (J/mol) \quad (5)$$

Also, the ratio of the partial pressures, s of Zn and Se_2 at the source is assumed not equal to the stoichiometric value of 2,

$$s = \frac{P_{Zn}(0)}{P_{Se_2}(0)} \neq 2. \quad (6)$$

Therefore, with s specified, the partial pressures $P_{Zn}(0)$ and $P_{Se_2}(0)$ can be found by solving (2), (4) and (6) and, with the total pressure assumed nearly constant, we have

$$P_t = P_{Zn}(0) + P_{Se_2}(0) \approx P_{Zn}(L) + P_{Se_2}(L). \quad (7)$$

We assume that there is no other species present in the source material, and we also assume that the effect of residual gases from the crucible is negligible for the model. The temperature profile is imposed by the furnace and will vary with x. Since the sublimation is an endothermic process, we must have T (L) smaller than T(0) if the material is to be transported from the source to the crystal. Thermo-physical data are obtained from refs. [35]. The interfaces are assumed to be flat for simplicity. The finite normal velocities at the interfaces can be expressed by Stefan flow deduced from the one-dimensional diffusion-limited model [36], which provide the coupling between the fluid dynamics and species calculations. On the other hand, the tangential component of the mass average velocity of the vapor at the interfaces vanishes. Thermodynamic equilibria are assumed at the interfaces so that the mass fractions at the interfaces are kept constant at $\omega_{A,s}$ and $\omega_{A,c}$. On the horizontal non-reacting walls an appropriate velocity boundary condition is no-slip, the normal concentration gradient is zero, and temperature is imposed as a linear temperature gradient or insulated.

Thermophysical properties of the fluid are assumed to be constant, except for the density. Instead of the Boussinesq approximation, the density is assumed to be a function of temperature and not of concentration. The ideal gas law and Dalton's law of partial pressures are used. Viscous energy dissipation and the Soret-Dufour (thermo-diffusion) effects can be neglected, as their contributions remain relatively insignificant for the conditions encountered in our PVT crystal growth processes. Radiative heat transfer can be neglected under our conditions, based on Kassemi and Duval [37].

3. Mathematical Formulation

The transport of fluid within a rectangular PVT crystal growth reactor is governed by a system of elliptic, coupled conservation equations for mass (continuity), momentum, energy and species (diffusion) with their appropriate boundary conditions. Let u_x, u_y denote the velocity components along the x- and y-coordinates in the x, y rectangular coordinate, and let T, ω_A, p denote the temperature, mass fraction of species A, Zn(g) and pressure, respectively.

The dimensionless variables are scaled as follows:

$$x^* = \frac{x}{H},\ y^* = \frac{y}{H}, \quad (8)$$

$$u = \frac{u_x}{U_c},\ v = \frac{u_y}{U_c},\ p = \frac{p}{\rho_c U_c^2}, \quad (9)$$

$$T^* = \frac{T-T_c}{T_s-T_c},\ \omega_A^* = \frac{\omega_A-\omega_{A,c}}{\omega_{A,s}-\omega_{A,c}}. \quad (10)$$

The dimensionless governing equations are given by:

$$\nabla^* \bullet V = 0, \quad (11)$$

$$\vec{V}\bullet\nabla^*\vec{V} = -\nabla^* p^* + Pr\cdot Ar\nabla^{*2}\vec{V} - Gr\cdot Pr^2\cdot Ar^2 T^*\cdot e_g, \quad (12)$$

$$\vec{V}\bullet\nabla^* T^* = Ar\nabla^{*2}T^*, \quad (13)$$

$$\vec{V}\bullet\nabla^*\omega_A^* = \frac{Ar}{Le}\nabla^{*2}\omega_A^*. \quad (14)$$

These nonlinear, coupled sets of equations are numerically integrated with the following boundary conditions:

On the source ($x^* = 0,\ 0 < y^* < 1$) :

$$u(0,y^*) = -\frac{Ar}{Le}\frac{1}{(v-1)}\frac{\partial\omega_A^*}{\partial x^*}, \quad (15)$$

$$u(0,y^*) = 0,$$

$$T^*(0,y^*) = 1,$$

$$\omega_A^*(0,y^*) = 1.$$

On the crystal ($x^* = L/H$, $0 < y^* < 1$) :

$$u(L/H, y^*) = \frac{Ar \Delta\omega}{Le\, C_v} \frac{\partial \omega_A^*}{\partial x^*}, \quad (16)$$

$$v(L/H, y^*) = 0,$$

$$T(L/H, y^*) = 0,$$

$$\omega_A^*(L/H, y^*) = 0.$$

Walls ($0 < x^* < L/H$, $y^* = 0$ and 1) :

$$u = v = \frac{\partial \omega_A^*}{\partial y^*} = 0, \quad (17)$$

$$T^*(x^*, 0) = T^*(x^*, 1) = -\frac{1}{Ar} \cdot x^* + 1$$

The governing dimensionless parameters are defined as

$$\text{thermal Grashoft number } Gr_t = \frac{g\beta_t \Delta T H^3}{\nu^2}, \quad (18)$$

$$\text{solutal Grashoft number } Gr_s = \frac{g\beta_s \Delta C H^3}{\nu^2}, \quad (19)$$

$$\text{aspect ratio } Ar = \frac{L}{H}, \quad (20)$$

$$\text{Prandtl number } Pr = \frac{C_P \mu}{\kappa}, \quad (21)$$

$$\text{Lewis number } Le = \frac{\kappa}{D_{AB}}, \quad (22)$$

$$\text{Peclet number } Pe = \frac{U_s L}{D_{AB}}. \quad (23)$$

$$\text{Concentration parameter } C_v = \frac{1/[1 + M_B/(2M_A)] - \omega_{A,c}}{\omega_{A,s} - \omega_{A,c}}. \quad (24)$$

The Peclet number can be also estimated by thermodynamic variables:

$$Pe \equiv \frac{U_s L}{D_{AB}} = \ln \frac{P_T - \frac{3}{2} P_A(L)}{P_T - \frac{3}{2} P_A(0)} \quad (25)$$

The analytical solution for the 1-D advective-diffusion model based on Stefan flow shows that the net mass flux is

$$J = \left(\frac{U_s P_T}{mRT}\right) = \frac{1}{m} \frac{D_{AB} P_T}{RT} \cdot \frac{1}{L} \ln \left[\frac{P_T/m - p_A(L)}{P_T/m - p_A(0)}\right] \quad (26)$$

where $m = 3/2$

U_{adv} is a characteristic velocity which depends on the thermodynamics of PVT processes, i.e., the vapor pressure of ZnSe as a function of temperature, which is termed as either an advective or a Stefan velocity. The mass fraction at the solid-vapor interfaces is fixed at the corresponding temperature. The definition of concentration parameter is found in refs. [33, 34]. In the dimensionless parameters in the governing equations the thermophysical properties of the gas mixture are estimated from gas kinetic theory using Chapman-Enskog's formulas [38]. The mass fraction at the source and crystal are calculated [31, 33] using the partial pressures and assuming ideal gas behavior as follows:

$$\omega_{Zn}(0) = \omega_s = \{1 + [P_{Se_2}(0) M_{Se_2}]/[P_{Zn}(0) M_{Zn}]\}^{-1} \quad \text{at } x = 0. \quad (27)$$

$$\omega_{Zn}(L) = \omega_c = \{1 + [P_{Se_2}(L) M_{Se_2}]/[P_{Zn}(L) M_{Zn}]\}^{-1} \quad \text{at } x = L. \quad (28)$$

The crystal growth rate v_c is calculated from a mass balance at the crystal vapor interface, assuming fast kinetics, i.e. all the vapor is incorporated into the crystal, which is given by (subscripts c, v refer to crystal and vapor respectively)

$$\int \rho_v u_v \cdot n dA = \int \rho_c u_c \cdot n dA, \quad (29)$$

$$V_c = \frac{\rho_v \int u_c \cdot n dA}{\rho_c \int dA}. \quad (30)$$

3. Results and Discussion

The parametric study is useful for showing trends and generalizing the problem, but many parameters are involved in the problem under consideration, which renders it difficult for a general analysis. One of the purposes for this study is to correlate the growth rate, for a particular material (ZnSe), to process parameters: (a) partial pressure ratio, s, and (b) temperature gradient across the ampoule. Thus, it is desirable to express some results in terms of dimensional growth rate, however they are also applicable to parameter ranges over which the process varies in the manner given. For this application, ranges of process parameters are typical for PVT processes under ground-based laboratory conditions. The six dimensionless parameters, namely Gr, Ar, Pr, Le, C_v and Pe, are independent and arise naturally from the dimensionless governing equations and boundary conditions. Because the precise values of s that correspond to the experiments are unknown, as a first step we assume values of s which are close to experimental growth conditions. Then we simulate diffusive-convective cases corresponding to actual experiments. The physical properties

Table 1
Typical thermo-physical properties used in simulations (M_{Zn} = 65.39, M_{Se_2} = 157.92)

Transport length, L	10 cm
Height, H	1.5 cm
Source temperature, T_s	1160°C
Crystal temperature, T_c	1130°C
Density, ρ	3.26×10^{-5} g/cm^3
Dynamic viscosity, μ	0.5×10^{-5} g/cm × sec
Diffusivity, D_{AB}	41.8 cm^2/s
Thermal expansion coefficient, β	6.98×10^{-4} K^{-1}
Prandtl number, Pr	0.76
Schmidt number, Sc	0.48
System stoichiometry (s)	0.2
Total system pressure, P_T	20.08 Torr
Zn partial pressure, source (s = 0.2)	3.35 Torr
Zn partial pressure, crystal (s = 0.2)	16.7 Torr
Se_2 partial pressure, source (s = 0.2)	2.17 Torr
Se_2 partial pressure, crystal (s = 0.2)	17.9 Torr

and operating conditions used in this study with s = 0.2 are listed in Table 1.

3.1. 1-D advective-diffusion model based on Stefan flow

We examine one-dimensional advective-diffusive case based on Stefan flow in order to understand the basic phenomena in the PVT process, which serves as numerics. The predictions based on 1-D advective-diffusive Stefan model have been thoroughly discussed in ref. [39]. The net mass flux for the 1D case is obtained by Eq. (26) and the dimensionless parameter Pe in (25) arises in the net mass flux. An 1-D analytical model based on Stefan flow shows a uniform streaming velocity from the source to the crystal [38]. Note that the 1-D

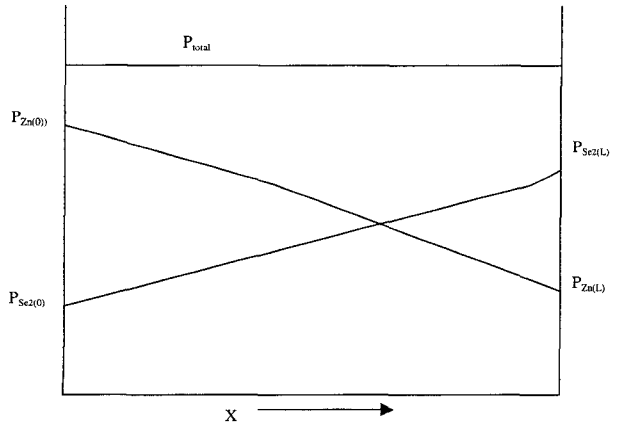

Fig. 2. Partial pressure profiles in the zinc-deficient vapor conditions with s < 2.

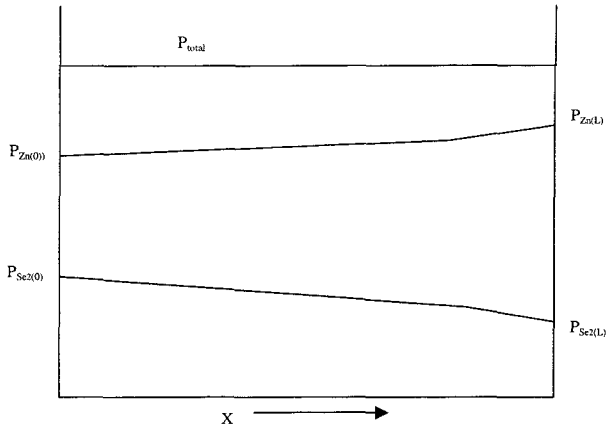

Fig. 3. Partial pressure profiles in the zinc-rich vapor conditions with s < 2.

case corresponds to the case simulated for the case when the zero-stress condition and Gr = 0 are employed.

Two typical partial pressure profiles are shown in Figs. 2 and 3 for the transport of vapor from the source to the crystal. Figs. 2 and 3 illustrates the case with s > 2 (Zn-rich vapor phase) and s < 2 (Zn-deficient vapor phase), respectively. Figs. 4 and 5 show the variation of Stefan velocity as a function of the temperature difference, ΔT between the source and crystal for various values of s (0.2 ≤ s ≤ 1.999: Zn-deficient vapor phase) and s (2.001 ≤ s ≤ 9 : Zn-rich vapor phase), respectively, with Ar = 6.67, H = 1.5 cm, L = 10 cm, and T_s = 1160°C. The Stefan velocity increases with both the partial pressure ratio s and the temperature difference, ΔT for 10 K ≤ T ≤ 50 K. For a given value of s, the Stefan velocity changes rapidly for small temperature differences up to 10 K, and increases with a constant and low gradi-

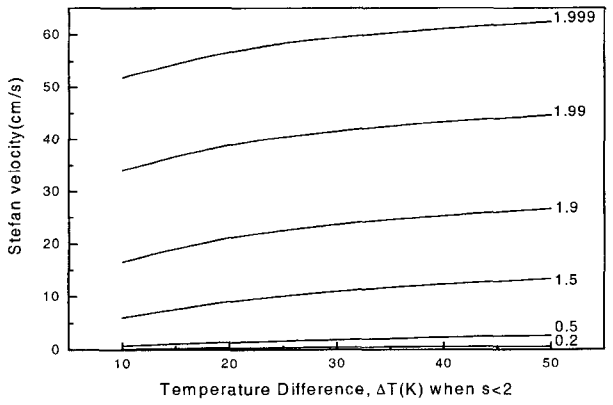

Fig. 4. Stefan velocity as a function of temperature difference, ΔT(K) between the source and crystal for various values of s (s < 2: Zn-deficient vapor conditions) with Ar = 6.67, H = 1.5 cm, L = 10 cm, and T_s = 1160°C. The Stefan velocity is predicted by the 1-D advective-diffusion model.

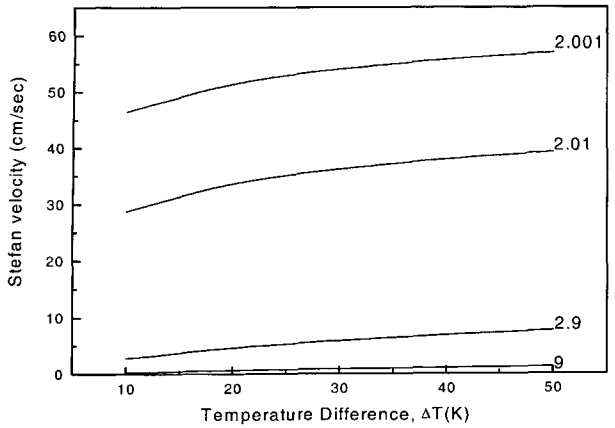

Fig. 5. Stefan velocity as a function of temperature difference, ΔT(K) for various values of s (s > 2: Zn-rich vapor conditions).

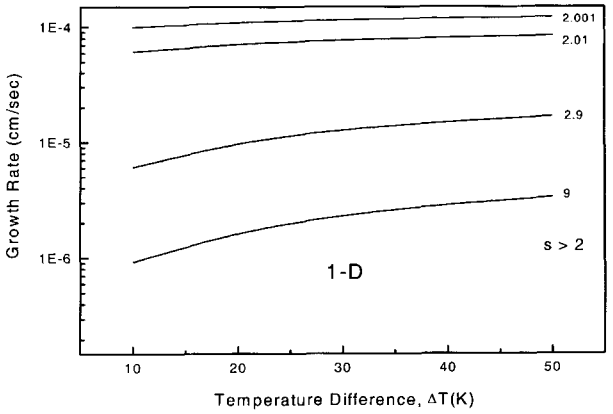

Fig. 7. The crystal growth rate of ZnSe as a function of temperature difference, ΔT(K) for Ar = 6.67, H = 1.5 cm, T_s = 1160°C, 2.001 ≤ s ≤ 9, based on the 1-D advection-diffusion (Stefan flow) model.

ent from 10 K to 50 K.

For the temperature ranges of 10 K ≤ ΔT ≤ 50 K, the Stefan velocity is increased by a factor of 3 for s = 0.2 and by a factor of 2 for s = 1.5. It indicates the Stefan velocity for low values of s is more sensitive to the temperature difference than for high values of s. With s = 0.2 the Stefan velocity gradient is 0.012 cm/s/K, while with s = 1.5 the corresponding gradient is 0.183 cm/s/K. The Stefan velocity gradient increases with the partial pressure ratio s. For the ratio s approaches 2, the variation of the Stefan velocity is large. Fig. 6 and 7 show the crystal growth rate of ZnSe as a function of temperature difference, ΔT(K), corresponding to Fig. 4 and 5, respectively. In Figs. 4 through 7 one sees that the closer to the stoichiometric case (s = 2), the larger is the growth rate and the Stefan velocity. It means the rate and velocity is much sensitive to the variation of s. Figure 5 shows the Stefan velocity for values lower than s

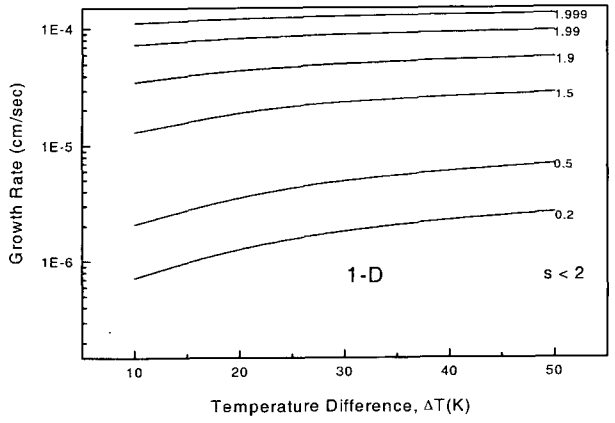

Fig. 6. The crystal growth rate of ZnSe as a function of temperature difference, ΔT(K) for Ar = 6.67, H = 1.5 cm, T_s = 1160°C, 0.2 ≤ s ≤ 1.999, based the 1-D advection-diffusion (Stefan flow) model.

= 3 have one order magnitude of velocity (cm/s) and as the ratio s increases, the velocity approaches zero. One sees in Fig. 6 that for 10 K ≤ ΔT ≤ 50 K, the rate for 1.999 ≤ s ≤ 1.5 have a range of 10^{-5} to 10^{-4} cm/s, but for 0.2 ≤ s < 1.5, a range of 10^{-5} to 10^{-6} cm/s. For s < 0.2, the rate has a value lower than approximately 10^{-6} cm/s. For ΔT = 10 K, the rate with s = 1.5 is greater than s = 0.2 by a factor of 4.69. On the other hand, at ΔT = 50 K, the former is greater than the latter by a factor of 3.67. It reflects that when ΔT is smaller, the larger is an increase in the rate with the ratio s. For the temperature differences closer to 50 K and the ratios of 1.5 < s < 1.999, the slope of growth rate versus ΔT is nearly variant. Therefore, a variation of the ratio s is a parameter more important than that of ΔT when ΔT is larger. At s = 1.999, the rate is nearly independent of ΔT. Similarly, at s = 2.001, the same result is obtained, as seen in Fig. 7. Note that as s → 2 the mechanism of PVT switches from dissociative sublimation to congruent sublimation as pointed out by Su and Sha [39]. Figure 7 that for 10 K ≤ ΔT ≤ 50 K, the rate for 2.001 ≤ s < 2.9 have a range of 10^{-5} to 10^{-4} cm/s, but for 2.9 ≤ s < 9, a range of 10^{-5} to 10^{-6} cm/s. For s < 9, the rate has a value lower than approximately 10^{-6} cm/s. For ΔT = 10 K, the rate with s = 9 is greater than s = 2.9 by a factor of 2.18. On the other hand, at ΔT = 50 K, the former is greater than the latter by a factor of 2.36. As a rule of thumb, in comparison with the case of s = 0.2 and 1.5 (s < 2), the case of s = 2.9 and 9 (s > 2) have little change in a factor based on the comparison of magnitude of the rate for two different ratios.

As the partial pressure ratio s approaches 2, the Stefan velocity approaches infinity [39]. This can be seen from boundary condition (15) since $C_v \rightarrow 1$ as s → 2

and hence u (dimensionless x-component velocity) $\rightarrow \infty$. It must be pointed out that this limiting behavior only serves to show a mathematical trend. Even though the velocity increases dramatically, it is bounded.

In order to operate near this singular case, we consider two kinds of values of s where the transport rate is limited by stichiometric variations that is either s > 2 (Zn-rich case) or s < 2 (Zn-deficient case). Evidently, the ratio s of the components in the vapor phase at the source material has a dramatic effect on the rate of transport. As seen in Figs. 4 through 7, the closer to the stoichiometric case, the larger is the Stefan velocity as well as the growth rate. Note that these figures are similar to the plots obtained using the 2D model, as shown later.

3.2. 2-D diffusive-convection model

In the experimental set-up, the cylinder is horizontally oriented with the hot temperature at the one side and the cold temperature at the other side. The cylinder has a diameter d = 1.5 cm and height H = 10 cm The source temperature T_s is 1160°C. The temperature profile along the side of cylinder is experimentally measured. A Zn-deficient case (s < 2) is considered to mimic the experimental conditions. We calculate the total pressure in the ampoule to be about 20 Torr. The system parameters for the 2-D diffusive-convection numerical computations are provided in Table 1. Typical calculations were performed for a stoichiometry parameter at the source s = 0.2 which is close to experimental growth conditions (Zn-deficient vapor phase). Figure 8 shows the growth rate as a function of temperature difference for two different models, 1-D Stefan and 2-D diffusive-convection model. The results show that for s = 0.2, 1-D case is slightly greater than the 2-D case for the temperature differences examined. The 2-D numerical predictions of crystal growth rates fall within the range of 1-D theoretical estimations. This reflects that for the growth conditions of ZnSe the flow fields would be 1-D advective-diffusive. For the temperature ranges of 10 K ≤ ΔT ≤ 50 K, the variations of growth rate with the temperature differences are nearly same for the two models, which supports the advective-diffusion is dominant over the flow fields within the growth enclosures. Figure 9 shows the growth rate as function of temperature difference for Ar = 6.67, H = 1.5 cm, T_s = 1160°C, s = 2.9, $0.366 \leq Pe \leq 1.00$, $4.65 \times 10^{-3} \leq Gr_t \leq 2.0 \times 10^{-2}$, $-8.5 \times 10^{-2} \leq Gr_s \leq -2.39 \times 10^{-2}$. s = 2.9 is chosen, which is close to experimental growth conditions (Zn-rich vapor phase) [34]. The trend similar to Fig. 8 is obtained, but the rate of 1-D case is greater than the 2-D by a factor of 3. The growth rate for the Zn-deficient case (s = 0.2) is greater than the Zn-rich case (s = 2.9) by approximately one order of magnitude, which is due to the effect of mass fluxes on the interfaces, i.e., sublimation and condensation. Therefore, the former has $0.04 \leq Pe \leq 0.16$ for the 10 K ≤ ΔT ≤ 50 K, while the latter has $0.366 \leq Pe \leq 1.00$. Figure 10. shows the maximum

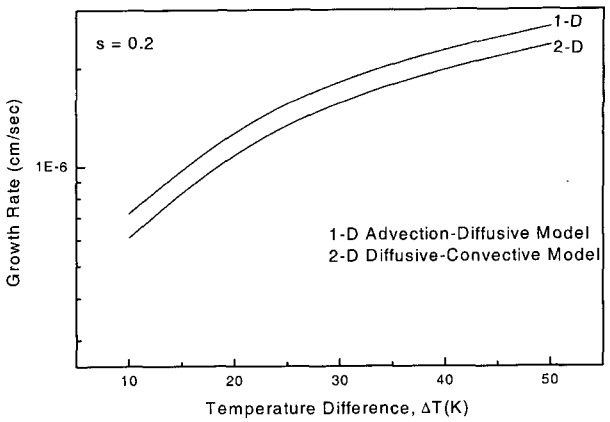

Fig. 8. The crystal growth rate of ZnSe as a function of temperature difference, ΔT(K) for Ar = 6.67, H = 1.5 cm, T_s = 1160°C, s = 0.2, $0.04 \leq Pe \leq 0.16$, $2.95 \times 10^{-6} \leq Gr_t \leq 0.056$, $4.62 \times 10^{-6} \leq Gr_s \leq 0.01$. For ΔT(K) = 10 K, Pe = 0.04, Gr_t = 0.056, Gr_s = 0.01; in the case of ΔT(K) = 10 K, Pe = 0.16, $Gr_t = 2.95 \times 10^{-6}$, $Gr_s = 4.62 \times 10^{-6}$. The broken line and solid lines represent the growth rate predicted by the 1-D advection-diffusion (Stefan flow) model and the 2-D numerical analysis based on the diffusion-limited model, respectively.

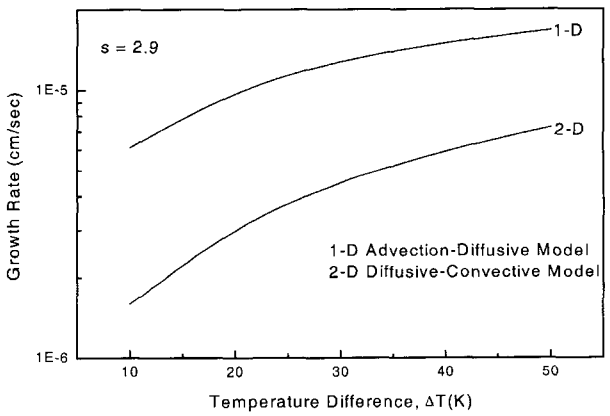

Fig. 9. The crystal growth rate of ZnSe as a function of temperature difference, ΔT(K) for Ar = 6.67, H = 1.5 cm, T_s = 1160°C, s = 2.9, $0.366 \leq Pe \leq 1.00$, $4.65 \times 10^{-3} \leq Gr_t \leq 2.0 \times 10^{-2}$, $-8.5 \times 10^{-2} \leq Gr_s \leq -2.39 \times 10^{-2}$. For ΔT(K) = 10 K, Pe = 0.366, $Gr_t = 4.65 \times 10^{-3}$, $Gr_s = -2.39 \times 10^{-2}$; in the case of ΔT(K) = 50 K, Pe = 1.00, $Gr_t = 2.0 \times 10^{-2}$, $Gr_s = -8.5 \times 10^{-2}$. The broken line and solid lines represent the growth rate predicted by the 1-D advection-diffusion (Stefan flow) model and the 2-D numerical analysis based on the diffusion-limited model, respectively.

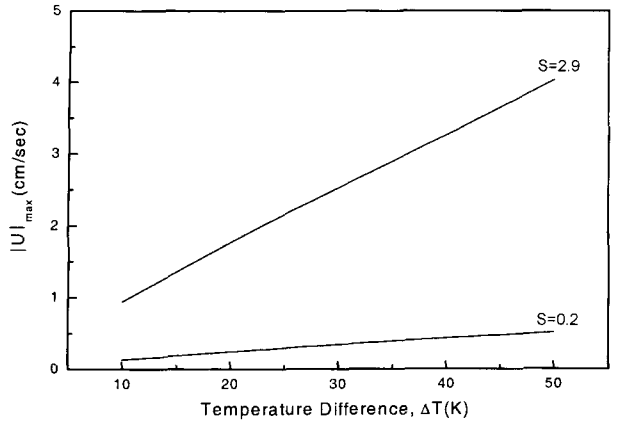

Fig. 10. The maximum magnitude of velocity, $|U|_{max}$ as a function of a function of temperature difference, ΔT(K) with s = 0.2 and 2.9, where $|U|_{max}$ as maximum magnitude of velocity vector represents an intensity of convection.

magnitude of velocity, $|U|_{max}$ as a function of a function of temperature difference, ΔT(K) with s = 0.2 and 2.9. $|U|_{max}$ as maximum magnitude of velocity vector represents an intensity of convection. Like the growth rate, the $|U|_{max}$ for the Zn-deficient case (s = 0.2) is greater than the Zn-rich case (s = 2.9) by one order of magnitude. The $|U|_{max}$ gradient of the temperature difference for s = 0.2 is 0.75 cm/sec/K, while that for s = 2.9 shows 0.075 cm/s/K.

Therefore, convection plays a role more important to the temperature variations for s = 2.9 than s = 0.2. Figure 11. shows the crystal growth rate of ZnSe as a Peclet number, Pe for s = 0.2 and 2.9, corresponding to Fig. 10. As mentioned previously, for 10 K ≤ ΔT ≤ 50 K, the Peclet number for s = 0.2 is varied from 0.04 to 0.16, while the Peclet number for s = 2.9 has a range of 0.366 ≤ Pe ≤ 1.00. The Peclet number for s = 0.2 is greater than that for s = 2.9 by one order of magnitude.

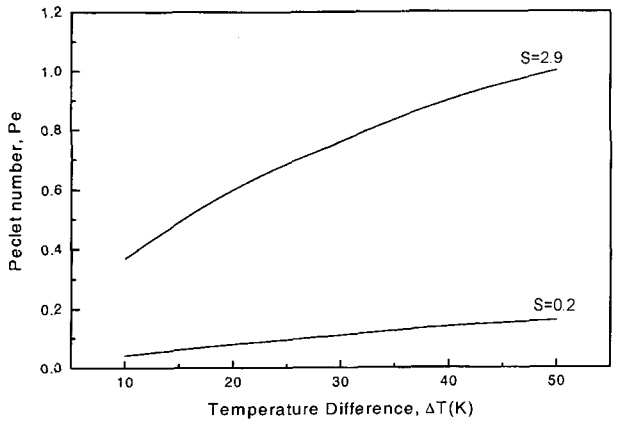

Fig. 11. The crystal growth rate of ZnSe as a Peclet number, Pe for s = 0.2 and 2.9, corresponding to Fig. 10.

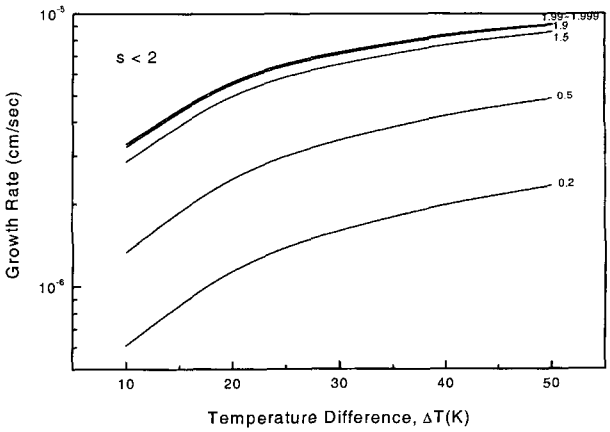

Fig. 12. The crystal growth rate of ZnSe as a function of temperature difference, ΔT(K) for Ar = 6.67, H = 1.5 cm, T_s = 1160°C, 0.2 ≤ s ≤ 1.999, 0.04 ≤ Pe ≤ 8.04, 0.04 ≤ Gr_t ≤ 0.056, 0.01 ≤ Gr_s ≤ 0.33, based on the 2-D numerical analysis based on the diffusion-limited model. For s = 0.2, Pe = 0.04, Gr_t = 0.056, Gr_s = 0.01; in the case of s = 1.999, Pe = 8.04, Gr_t = 0.04, Gr_s = 0.33.

Therefore, it is clear that the Peclet number is directly related to the $|U|_{max}$ so that the $|U|_{max}$ increases as the Peclet number increases.

Figure 12 shows the crystal growth rate of ZnSe as a function of temperature difference, ΔT(K) for Ar = 6.67, H = 1.5 cm, T_s = 1160°C, 0.2 ≤ s ≤ 1.999, 0.04 ≤ Pe ≤ 8.04, 0.04 ≤ Gr_t ≤ 0.056, 0.01 ≤ Gr_s ≤ 0.33, based on the 2-D numerical analysis based on the diffusion-limited model. The curves for 0.2 ≤ s ≤ 1.999 have similar profiles for the temperature differences examined, 10 K ≤ ΔT ≤ 50 K, which indicates the same variation of the rate over the temperature difference. As the value of the ratio of partial pressure approaches the stoichiometric value, s = 2 from s = 0.5, the rate increases sharply.

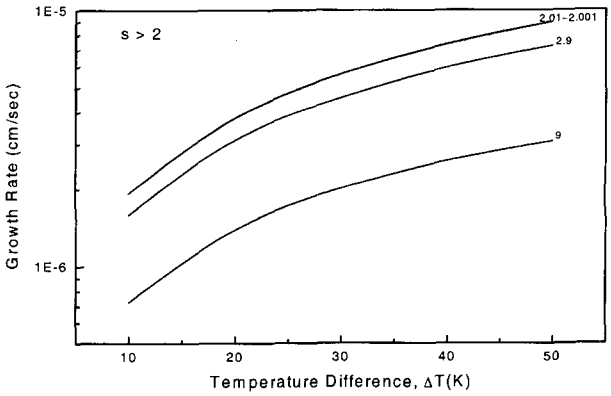

Fig. 13. The crystal growth rate of ZnSe as a function of temperature difference, ΔT(K) for Ar = 6.67, H = 1.5 cm, T_s = 1160°C, 2.001 ≤ s ≤ 9, 0.2 ≤ Pe ≤ 7.35, Gr_t = 0.02, –0.039 ≤ Gr_s ≤ –0.12, based on the 2-D numerical analysis based on the diffusion-limited model. For s = 2.001, Pe = 7.35, Gr_t = 0.02, Gr_s = –0.12; for s = 9, Pe = 0.2, Gr_t = 0.02, Gr_s = –0.039.

From s = 1.5 to 1.999, the rate are slightly varied. Figure 13 shows the crystal growth rate of ZnSe as a function of temperature difference, $\Delta T(K)$ for $2.001 \leq s \leq 9$. As the value of the ratio of partial pressure approaches the stoichiometric value, s = 2 from s = 9, the rate increases sharply. From s = 9 to 2.001, the rate are slightly varied.. As seen in Figs. 12 and 13, the similar profiles of the rate are obtained for s = 0.2 and 2.9,except for the difference of the rate by one order of magnitude between s = 0.2 and 2. Again we find that the growth rate increases with the partial pressure ratio s. Convection is also very weak and steady. As expected, the growth rate is still very close to that of the Stefan flow case. In order to study the effect of gravitational accelerations on the rate, the gravitational constant is varied from 1 g to 10^{-6} g, the rate remains nearly constant. Therefore, diffusive-convection is independent of gravity. In other words, reducing the gravitational level such that $Gr \rightarrow 0$, as provided by microgravity environments, would not affect the diffusive-convection flow fields for low vapor pressure system such as ZnSe vapor growth processes.

4. Conclusions

For the study of diffusive-convection in the ZnSe crystal growth processes by PVT with dissociative sublimation, the effects of the processes parameters such as the temperature difference, the gravitational level on the crystal growth are computationally investigated. of the ratio of partial pressures. The Stefan velocity increases with both the partial pressure ratio s and the temperature difference, ΔT for $10\ K \leq \Delta T \leq 50\ K$. For a given value of *s*, the Stefan velocity changes rapidly for small temperature differences up to 10 K, and increases with a constant and low gradient from 10 K to 50 K. The curves for $0.2 \leq s \leq 1.999$ have similar profiles for the temperature differences examined, $10\ K \leq \Delta T \leq 50\ K$, which indicates the same variation of the rate over the temperature difference. As the value of the ratio of partial pressure approaches the stoichiometric value, s = 2 from s = 0.5, the rate increases sharply. As the value of the ratio of partial pressure approaches the stoichiometric value, s = 2 from s = 0.5, the rate increases sharply. From s = 1.5 to 1.999, the rate are slightly varied. the similar profiles of the rate are obtained for s = 0.2 and 2.9, except for the difference of the rate by one order of magnitude between s = 0.2 and 2. Our results show that for the ratios of partial pressures, s = 0.2 and 2.9, the growth rate increases with the Peclet number and the temperature differences between the source and crystal. As the ratio of partial pressures approaches the stoichiometric value of 2, the rate increases. The mass flux based on one dimensional (1D model) flow for low vapor pressure system fall within the range of the predictions (2D model) obtained by solving the coupled set of conservation equations, which indicates the flow fields would be advective-diffusive. Therefore, the rate and the flow fields is independent of gravity acceleration levels.

Acknowledgement

This work was financially supported by Korea Science and Engineering Foundation (KOSEF) under the project number 2001-1-30700-009-2 in 2001.

Nomenclature

A	: component A, Zn(g)
B	: component B, Se_2(g)
D_{AB}	: diffusivity of A and B
e_g	: unit vector of gravity acceleration
g	: standard gravitational acceleration constant, 980.665 cm/s^2
H	: height (cm)
L	: transport length (cm)
M	: mean molecular weight of component A and B
P	: pressure
P_T	: total pressure
R_g	: ideal gas constant
T	: temperature
ΔT	: temperature difference between source and crystal, $T_s - T_c$
$\Delta\omega$	: mass fraction difference between source and crystal, $\omega_{A,s} - \omega_{A,c}$
x	: x-coordinate
y	: y-coordinate
u	: dimensionless x-component velocity
U_{adv}	: characteristic velocity based on the diffusive-advective flux
U_c	: characteristic velocity, κ/H
$\|U\|_{max}$	: dimensional maximum magnitude of velocity vector
v	: dimensionless y-component velocity
u_x	: x-component velocity

u_y : y-component velocity
V : velocity vector
V_c : growth rate

Dimensionless Governing Parameters

Ar : aspect ratio, L/H
C_v : concentration parameter, $C_v = (1 - \omega_{A,c})/\Delta\omega$
Le : Lewis number, κ/D_{AB}
Pe : Peclet number, $U_{adv}L/D_{AB}$
Pr : Prandtl number, ν/κ
Gr : Grashof number, $g\beta\Delta TL^3/\nu^2$

Subscripts and Superscripts

A : component A, Zn(g)
Adv : advection
B : component B, Se_2(g)
c : crystal
s : source
T : total vapor pressure
* : dimensionless

Greek Letters

β : thermal volume expansion
κ : thermal diffusivity
ν : kinematic viscosity
∇^* : $(\partial/\partial x^*) + (\partial/\partial y^*)$
∇^{*2} : $(\partial^2/\partial x^{*2}) + (\partial^2/\partial y^{*2})$
ϕ : variable (u, v, T*, ω_A^*)
ω : mass fraction meaning dimensionless mass concentration density of fluid with component A and B

References

[1] H. Kukimoto, "Conductivity control of ZnSe grown by MOVPE and its application for blue electroluminescence," J. Crystal Growth 101 (1990) 953.
[2] H.J. Eichler, V. Glaw, A. Kummrow, V. Penschke and Wahi, "Optically bistable thin film devices using wide-gap II-VI compounds," J. Crystal Growth 101 (1990) 695.
[3] S. Guha, J.M. DePuydt, M.A. Hasse, J. Qiu and H. Cheng, Appl. Phys. Lett. 63 (1993) 3107.
[4] M.A. Hasse, J.M. DePuydt and H. Chen, Appl. Phys. Lett. 59 (1991) 1272.
[5] H. Jeon, J. Ding, A.V. Nurmikko, W. Xie, D.C. Grillo, M. Kobayashi, R.L. Gunshor, G.C. Hua and N. Otsuka, Appl. Phys. Lett. 60 (1992) 2045.
[6] W.C. Holton, R.K. Watts and R.D. Stinedurf, Eichler, J. Crystal Growth 6 (1969) 97.
[7] M.J. Kozielski, "Polytype single crystals of $Zn_{1-x}Cd_xS$ and $ZnS_{1-x}Se_x$ solid solutions grown from the melt under high argon pressure by bridgmans method," J. Crystal Growth 30 (1975) 86.
[8] I. Kikuma, and M. Furukoshi, "Melt growth of ZnSe crystals under argon pressures," J. Crystal Growth 41 (1977) 103.
[9] C.C. Chang, C.C. Wei, Y.K. Su and H.C. Tzeng, "Growth and characterization of ZnSe single crystals by closed tube methods," J. Crystal Growth 84 (1987) 11.
[10] K. Mochizuki, K. Masumoto and H. Iwanaga, "Morphology and photoluminescence (PL) of ZnSe single crystals grown frm Se and/or as solvents," J. Crystal Growth 84 (1987) 1.
[11] H. Hartmann, "Studies on the vapour growth of ZnS, ZnSe and ZnTe single crystals," J. Crystal Growth 42 (1977) 144.
[12] W. Palosz, "Growth of ZnS and $Zn_{1-x}Cd_xS(x < 0.07)$ single crystas by iodine transport," J. Crystal Growth 60 (1982) 57.
[13] K. Böttcher and H. Hartmann, "Zinc selenide single crystal growth by chemical transport reactions", J. Crystal Growth 146 (1995) 53.
[14] J.R. Cutter and J. Woods, "Growth of single crystals of zinc selenide from the vapor phase", J. Crystal Growth 47 (1979) 405.
[15] H.Y. Cheng and E.E. Anderson, "The growth of ZnSe single crystals by physical vapor transport", J. Crystal Growth 96 (1989) 756.
[16] Yu. U. Korostelin, V.I. Kozlovsky, A.S. Nasibov and P.V. Shapkin, "Vapour and characterization of bulk ZnSe single crystals", J. Crystal Growth 161 (1996) 51.
[17] C.H. Su, S. Feth and S. L. Lehoczky, "In situ partial pressure measurements and visual observation during crystal growth of ZnSe by seeded physical vapor transport", J. Crystal Growth 209 (2000) 687.
[18] C.H. Su, M.A. George, W. Palosz, S. Feth, S.L. Lehoczky, "Contactless growth of ZnSe single crystals by physical vapor transport", J. Crystal Growth 213 (2000) 267.
[19] C.H. Su, S. Feth, L. J. Wang and S. L. Lehoczky, "Photoluminescene studies of ZnSe starting materials and vapor grown bulk crystals", J. Crystal Growth 224 (2001) 32.
[20] F. Rosenberger, "Fluid dynamics in crystal growth from vapors", Physico-Chemical Hydro-dynamics 1 (1980) 3.
[21] M.M. Faktor and I. Garrett, Growth of Crystals from the Vapour, (Chapman & Hall, London, 1974).
[22] Y.-G. Sha, C.-H. Su, W. Palosz, M.P. Volz, D.C. Gillies, F.R. Szofran, S.L. Lehoczky, H.-C. Liu and R.F. Brebrick, "Mass flux of ZnSe by physical vapor transport", J. Crystal Growth 146 (1995) 42.
[23] C.-H. Su, "Growth rate of CdS by vapor transport in closed ampoule," J. Crystal Growth 80 (1987) 333.
[24] D.W.G. Ballentyne, S. Wetwatana and E.A.D. White, J. Crystal Growth 7 (1979) 79.
[25] B.L. Markham, D.W. Greenwell and F. Rosenberger, "Numerical modeling of diffusive-convective physical vapor transport in cylindrical vertical ampoules", J. Crystal Growth 51 (1981) 426.

[26] Walter M.B. Duval, "Transition to chaos in the physical transport process--I", the Proceeding of the ASME--WAM Winter Annual meeting, Fluid mechanics phenomena in microgravity, ASME-WAM, New Orleans, Louisiana, Nov. 28 -- Dec. 3, AMD-174, FED-175 (1993) 51.
[27] W.M.B. Duval, "Convection in the physical vapor transport process-- II: Thermosolutal convection", J. Chem. Vapor Deposition 2 (1994b) 282.
[28] W.M.B. Duval, "Convection in the physical vapor transport process-- I: Thermal convection", J. Chem. Vapor Deposition 2 (1994a) 188.
[29] A. Nadarajah, F. Rosenberger and J. Alexander., "Effects of buoyancy-driven flow and thermal boundary conditions on physical vapor transport", J. Crystal Growth 118 (1992) 49.
[30] F. Rosenberger, J. Ouazzani, I. Viohl and N. Buchan, "Physical vapor transport revised", J. Crystal Growth 171 (1997) 270.
[31] G.T. Kim, W.M. B Duval, M. E. Glicksman and N.B. Singh, "Thermal convective effects on physical vapor transport growth of mercurous chloride (Hg_2Cl_2) crystals for axisymmetric 2D cylindrical enclosure", Modelling Simul. Mater. Sci. Eng. 3 (1995) 331.
[32] S.K. Kim, S. Y. Son, K. S. Song, J.-G. Choi and G. T. Kim, "Mercurous bromide (Hg_2Br_2) crystal growth by physical vapor transport and characterization", J. Korean Crystal Growth and Crystal Technology 12, 6 (1995) 272.
[33] H. Zhou, A. Zebib, S. Trivedi and W.M.B. Duval, "Physical vapor transport of zinc-telluride by dissociative sublimation", J. Crystal Growth 167 (1996) 534.
[34] N. Ramachandran, C.H. Su and S.L. Lehoczky, "Modeling studies of PVT growth of ZnSe: current status and future course", J. Crystal Growth 208 (2000) 269.
[35] R.F. Brebrick and H.-C. Liu, High Temp. Mater. Sci. 35 (1996) 215.
[36] F. Rosenberger and G. Muller, "Interfacial transport in crystal growth, a parameter comparison of convective effects", J. Crystal Growth 65 (1983) 91.
[37] M. Kassemi and Walter M.B. Duval, "Interaction of surface radiation with convection in crystal growth by physical vapor transport", J. Thermophys. Heat Transfer 4 (1989) 454.
[38] R.C. Reid, J.M. Prausnitz, B.E. Poling, Bird, The properties of gases & liquids (McGraw-Hill, New York, NY, 1988).
[39] C.H. Su and Y.G. Sha, Current topics in Crystal Growth Research, edited by the council of scientific information to be published by researched trends.
[40] H. Wiedemeier, D. Chandra and F.C. Klaessig, "Diffusive and Convective Vapor Transport in the GeSe-GeI_4 system", J. Crystal Growth 51(1980) 345-361.

APPENDIX

The transport coefficients are estimated using Chapman-Enskog's formulas. These formulas are based on kinetic theory of gases at low density and uses a molecular force field model. In this model the potential energy of interaction (Φ) between two molecules separated by a distance r is related to the force of interaction (F), via $\Phi = -d\Phi/dr$. Since F is not known exactly, the Lennard-Jones (6-12) empirical potential function is used to derive formulas for the transport coefficients, i.e.,

$$\Phi(r) = 4\varepsilon\left[\left(\frac{\sigma}{r}\right)^{12} - \left(\frac{\sigma}{r}\right)^{6}\right]. \tag{A1}$$

Note σ and ε are tabulated values; they may also be estimated from the properties of the fluid. For Zn(g) and Se2(g), σ and ε are estimated from the properties of the solid at the melting point as follow:

$$\varepsilon/\kappa = 1.92T_m \quad \sigma = 1.22V_{m,sol}^{1/3} \tag{A2}$$

The melting points of Zn and Se are 419.58°C and 217°C, respectively. The ó for the Zn and Se are 2.43 Å and 3.91 Å.

Viscosity

The viscosity of Zn(g) and Se_2(g) are estimated from the formula for a monatonic gas,

$$\mu = \frac{2.66693\times10^{-5}\sqrt{MT}}{\sigma^2\Omega_\mu} \tag{A3}$$

$$\Omega_\mu = \frac{A}{T^{*B}} + \frac{C}{\exp(DT^*)} + \frac{E}{\exp(FT^*)} \tag{A4}$$

where $T^* = \kappa T/\varepsilon$ and A = 1.16145, B = 0.14874, C = 0.52487, D = 0.77320, E = 2.16178, F = 2.43787, see [38]. Ω_μ is a function which represents the deviation from rigid sphere behavior. The gas mixture viscosity is calculated using:

$$\mu_{mix} = \sum_{i=1}^{n} \frac{x_i\mu_i}{\sum_{j=1}^{n} x_i\Phi_{ij}} \tag{A5}$$

$$\Phi_{ij} = \frac{1}{\sqrt{8}}\left(1 + \frac{M_i}{M_j}\right)^{-1/2} \tag{A6}$$

where n is the number of chemical species in the mixture. The mixture viscosity is evaluated from:

$$\nu_{mix} = \mu_{mix}/\rho \tag{A7}$$

where

$$\rho = \sum_{i=1}^{n} \frac{P_iM_i}{RT} \tag{A8}$$

Thermal Conductivity

The thermal conductivity is calculated similarly to the viscosity, for a monatomic gas

$$\kappa = 1.9891\times10^{-4}\frac{\sqrt{T/M}}{\sigma^2\Omega_\kappa}. \tag{A9}$$

Since $\Omega_\mu = \Omega_\kappa$, the same correlation as above can be used. The thermal conductivity for a monatomic gas can also be estimated from the viscosity using

$$\kappa = \frac{15}{4}\frac{R}{M}\mu = \frac{5}{2}C_v\mu. \tag{A10}$$

For a polyatomic gas, k is given by

$$\kappa = \left(C_p + \frac{5}{4}R\right)\frac{\mu}{M} \tag{A11}$$

For a gas mixture,

$$\kappa_{mix} = \sum_{i=1}^{n}\frac{x_i k_i}{\sum_{j=1}^{n} x_i\Phi_{ij}} \tag{A12}$$

where Φ_{ij} is the same as above. The thermal diffusivity of the gas mixture of Zn(g) and Se_2(g) is evaluated using,

$$\alpha_{mix} = \kappa_{mix}/\rho C_{pmix} \quad C_{pmix} = x_i C_p \tag{A13}$$

For Se_2(g),

$$Cp = A + B\cdot 10^5 T^{-2} \tag{A14}$$

where A = 8.94, B = –0.43 [40].

Mass Diffusivity for Binary Mixtures

The diffusion coefficient for the mixture is estimated from,

$$D_{AB} = 0.0018583\frac{\sqrt{T^3\left(\frac{1}{M_A}+\frac{1}{M_B}\right)}}{p\sigma_{AB}^2\Omega_{D,AB}} \tag{A15}$$

where

$$\varepsilon_{AB} = \sqrt{\varepsilon_A\varepsilon_B},\ \sigma_{AB} = 1/2(\sigma_A + \sigma_B) \tag{A16}$$

The function $\Omega_{D,AB}$ [13] may be estimated from:

$$\Omega_{D,AB} = \frac{A}{T^{*B}} + \frac{C}{\exp(DT^*)} + \frac{E}{\exp(FT^*)} + \frac{G}{\exp(HT^*)} \tag{A17}$$

where $T^* = \kappa T/\varepsilon_{AB}$ and A = 1.06036, B = 0.15610, C = .19300, D = 0.47635, E = 1.03587, F = 1.52996, G = 1.76474, H = 3.89411.